International Journal of Applied Engineering Research ISSN 0973-4562 Volume 13, Number 15 (2018) pp. 12318-12325

An Improved Method of Measuring Spatial Resolution of the Computed Tomography from ESF based on CT phantom images

Almahdi M. Alshweikh[1], Kus Kusminarto[2] ,Gede B. Suparta[3]

[1]*Atomic physics laboratory, Department of Physics, Gadjah Mada University, Yogyakarta, 55281, Indonesia.*

[2,3] *Department of Physics, Gadjah Mada University, Yogyakarta, 55281, Indonesia.*

[1]*Orcid: 0000-0003-3492-3703,*

Abstract

Spatial resolution is an important feature of the computed tomography (CT) imaging system, which is the ability of an image to convey details and distinguish between small objects that are close together. In this paper, a simple developed methodology for measuring the spatial resolution of CT images is implemented using phantom images. The present study offers an alternative methodology to the measurement of the spatial resolution of CT machine which is based on the calculation of the full width at half maximum (FWHM) of the line spread function (LSF) acquired from a function called the edge spread function (ESF). The ESFs data were constructed from the CT image obtained by scanning phantom made of silicone rubber shaped as a cylindrical containing different material. The ESF curves were obtained by a direct fit of a mathematical expression of the ESF profile using MATLAB (R2015b) to the ESF data acquired at the interface between the different materials within the experiment phantom. The proposed methodology can be implemented using signal data from the reconstructed CT image and is not sensitive to the noise introduced by differentiating the ESF to produce the LSF as noted in the previous measurement. In addition, the proposed methodology provides a practical measurement of CT machine spatial resolution.

Keyword: Micro- Computed Tomography, Spatial resolution, Edge spread function (ESF), full width at half maximum (Fwhm).

INTRODUCTION

Computed Tomography (CT) is a non-invasive imaging system that produces cross-sectional images of an object from 2D X-ray projections [1, 2]. CT machine was first developed in the 1970's and has since become an important imaging modality for a doctor to diagnose and treat a wide range of diseases [3, 4, 5]. CT has been widely used in medical imaging, and many other fields. Through its applications, medical diagnosis is the most common [6].

A microscopic computed tomography (Micro-CT) is, in principle, a small version of clinical CT, which can produce voxel sizes in the final 3D image within the micrometer scale [2]. Recently it has become possible to construct CT systems that can deliver such high resolution. Micro-CT has been commonly used in preclinical examinations such as scans of tissue samples, organs or small animals that are used as models to evaluate human diseases and therapies [7, 8]. It has also been used for material testing and analysis, as well as a tool for indirect approaches to molecular imaging [9]. The Micro-CT system which is used in this research was developed by the Physics of Imaging Research Group (PIRG) Department of Physics, University of Gadjah Mada [10].

The image quality of CT system is characterized by several parameters such as resolution which includes spatial resolution, contrast resolution, and temporal resolution [11, 12]. Resolution is the important feature of the image quality which can be defined as the ability of CT imaging system to discriminate between small objects that are close together [11, 13]. Good CT image resolution clarifies accurate anatomic structures and details. It is measured in line (pairs per millimeter), which refers to the ability of a CT system to show that very small pairs of lines are separated lines and not a single line. In an ideal condition, spatial resolution describes the size of the smallest objects that can be separately discriminated by an imaging system. However, the effects of contrast resolution and noise are very influential, so a proper description of spatial resolution needs to incorporate these factors [11].

Spatial resolution of CT machine can be measured by direct (lp/mm) or by using modulation transfer function (MTF) [14]. To measure it directly, a line pair's phantom is used. This phantom is made of acrylic (PMMA) and has closely spaced metal strips. After scanning the phantom, the numbers of strips that are visible are counted. A line pair is not a set of two lines, but rather a line and the space between the lines. [14]. The MTF can be defined as the ratio of the output modulation to the input modulation; it measures the response of a system to different frequencies. MTF is an important quantities parameter to assess the spatial resolution of a CT system, which has been widely used by the previous researchers [15, 16, 17]. Common methods to measure the MTF of a CT system include using a line-pair pattern phantom [16] and a thin metal wire [18]. In this process, the MTF curves can be obtained from the reconstructed phantom image of a thin wire based on the fact that MTF is the magnitude of the Fourier transformation of the point spread function (PSF) [6].

Hence, there are a number of studies in determining the spatial resolution of CT system such as. Rainer [17] proposed and evaluated a new method for analyzing the spatial resolution of CT data from only a single scan. He assists the PSF and the modulation transfer function (MTF) of a CT

scanner using a single measurement in the wire phantom he stated that the wire method does not allow to assess the longitudinal point spread function and proposed to measure a sphere, performed a standard image reconstruction and evaluated profiles through the sphere surface. The radial symmetry of CT scanners allows reducing the dimensionality of the PSF and the MTF from three to two by radial averaging.

Rong Jun *et al.,* [19] measured the spatial resolution of Micro-CT system using test phantom of the aluminum cylinder based on the MTF. The MTF was determined by computing the amplitude of the Fourier transform of the line spread function (LSF) which was obtained by calculating the derivative of the edge profile of cylindrical phantom called edge response function (ERF). The ERF was calculated based on the reconstruction image finally; they stated that the tungsten wire used in the experiment could be detected by the system which influenced by the projections and the pixel number. Judy [20] measured the LSF directly using phantom made from the thin object embedded in a water bath, the estimate of the LSF was not precise because the thin object had significantly larger linear attenuation coefficient than water. Artifacts were observed when small high contrast object was scanned. Boone [21] suggested that the measurement of spatial resolution by using LSF phantom, which built with a thin aluminum foil sandwiched between two slabs of acrylic; it will affect the CT image because of the presence of a high attenuation metal foil. Bentzen [22] presented a new approach to the measurement of the spatial resolution of CT scanner system. Based on a direct least squares using thin wire phantom his data was obtained from the CT image of interface between two materials and stated that the spatial resolution may be described by the full width at half maximum (FWHM) of the line spread function obtained from scanning the wire phantom. The main drawback of using wire phantom is the limited number of data points available for the determination of the FWHM due to the rather rough grid of pixels in the CT image output matrix.

ICRU Report 87 [23] mentioned that the PSF, LSF, and the ESF were used to measure spatial resolution of computed tomography. In relation to the phantom design, these methods utilized with phantoms made of thin medal foil have some drawbacks or weaknesses for example the PSF method. The PSF is difficult to determine in practice because an infinitesimal point object cannot be produced perfectly. It can only be approximated. Another method is through the LSF, which is the distribution of pixel intensities in the image of a long, narrow slit of the unit intensity. The LSF can be obtained by imaging a narrow slit, but this is impractical since it is impossible to obtain an infinitely thin line source or a narrow slit [24].

These mentioned studies above showed that the measured spatial resolution was still having some point of weakness. Instead, practical imaging systems such as CT are advisable by the FWHM of an image produced from a small point object or the width of the LSF which is derived from the ESF. The LSF and ESF are viewed as experimental tools for determining the FWHM of the CT system. Since the FWHM was linked to the LSF, the LSF was acquired practically in this experiment. This was realized by imaging phantom cylindrical shape, with an internal cavity containing four different materials arranged side by side to achieve the spread of the discontinuity of the image which refers to the ESF.

The aim of this work presented in this paper was to introduce and explain an alternative methodology to the measurement of the spatial resolution of CT machine. The proposed methodology is based on measurement the FWHM of the LSF which is calculated from a related function called the ESF. The ESF data were constructed from the CT image which was obtained by scanning phantom containing different materials with different linear attenuation coefficient (μ). The ESF obtained by a direct fit of a mathematical expression of the ESF profile using MATLAB (R2015b) to the ESF data acquired at the interface between the different materials within the experiment phantom. The proposed methodology can be implemented using signal data from the reconstructed CT image and is not sensitive to the noise introduced by differentiating the ESF to produce the LSF as noted in the previous measurement. In addition, the proposed methodology provides a practical measurement of CT machine spatial resolution.

MATERIALS AND METHODS

1. EQUIPMENT

A developed micro computed tomography system (μ- DRCT Scan) was used in this study. The complete setup of the experiment is contained in a shielding hutch. Inside the hutch, there is an X-ray tube, a phantom mount on top of a rotation stage, and an X-ray detector; all components are connected to a computer outside the hutch to control the experiment. The X-ray tube and the detector are placed opposite each other at a distance of 150 mm. The X-ray tube is a 'PHILIPS TYPE PW2215/20 that has a molybdenum target capable of a range from 20 to 60 keV with a maximum beam current of 30 mAs and a maximum power of 2000, the rotation stage installed between the X-ray source and the detector providing full rotation of the experiment object. The detector inside the experiment setup is CMOS digital camera and fluorescence Scintillator. It has an active area of 2 cm and Pixel spacing $48\mu m$, used to receive the attenuated profile as raw information for the reconstruction process. Besides, a computer control system is used to control the X-ray source and the scanning parameters as well as performing reconstruction software to transform the radiographic images to the interior volumetric view of the phantom.

The experiment phantom was scanned by the Micro-CT system with 30 keV X-ray energy and 20 mA tube current. The phantom was placed on the top of the rotation stage as illustrated in Figure 1 continued with scanning the phantom. The scanning process was running from 0 to 359 degree collated three-radiograph image for each projection angle. Each of the three-radiograph images was processed to generate only one radiograph image using the software. The software DRCT created the sinogram from the radiograph image based on the radiograph image selected. The resulting sinogram was reconstructed employing a reconstruction

algorithm provided by the DRCT software with standard filtered-back projection technique to produce the CT scan image which was used to evaluate the spatial resolution of the system.

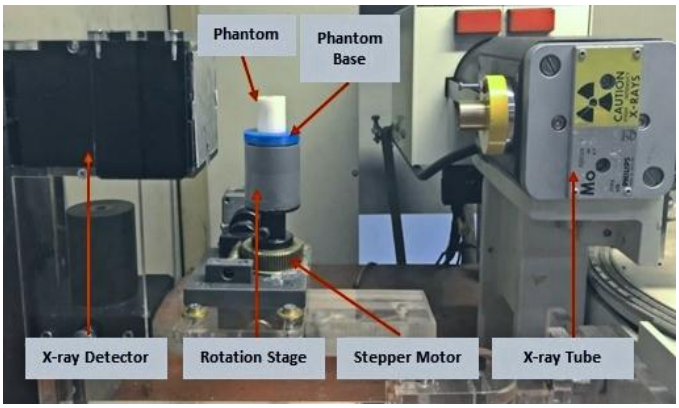

Figure 1: Schematic picture of experimental arrangement

2. PHANTOM DESIGN AND FABRICATION

The ESF provides obvious practical advantages compared with the LSF method. First, an edge used to measure ESF is easier to fabricate than a narrow slit employed in the LSF measurement [25]. Second, the measurement is in the same form as the image information is determined. In fact, the main reason for the known system resolution is to distinguish how the edges in an image are blurred. A developed multi-materials phantom was used in this study to measure the LSF curves for the spatial resolution measurements. The factors were considered for the phantom design is geometry, dimensions, and materials. The general concept of the phantom design was a cylindrical shape made of silicone rubber material by molding the silicone into a template made of PLA plastic using 3D printer. The dimensions of the cylinder were 1.7cm diameter and 2cm height with an internal rectangular cavity made inside the cylinder to insert the different density materials as shown in Figure 2.

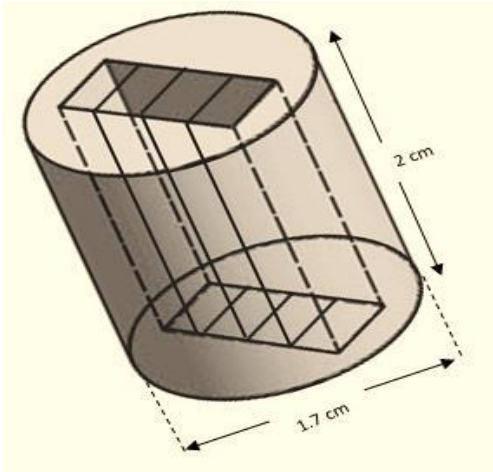

Figure 2: Design of the multi-materials phantom

The internal cavity shaped in 3D rectangular with a height of 2 cm, length of 12 mm, and width of 5 mm the cavity was divided into four parts with 3 mm for each part to insert the different materials. The materials which were selected to be inserted inside the cavity were Plexiglas, soap (Sodium Palmate), paraffin, and plastic materials. The four colors in Figure 3 shows the four kinds of materials placed inside the phantom side by side to provide the edge required for the measurements.

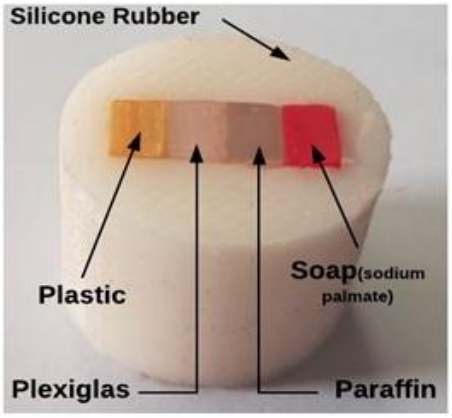

Figure 3: phantom used in this study

3. EXPERIMENTAL PROCEDURE

Preceding study has used a wire phantom to assess the spatial resolution of the CT system by scanning the phantom to achieve the LSF, on the condition that the LSF can be approximated by a Gaussian function from the reconstructed CT image. However, this case of study is limited to the number of data points available for the determination of the LSF due to the rather rough grid of pixels in the CT image output matrix. Instead, the experiment described in this paper proposes that the LSF can be derived from the ESF by numerical differentiation. The ESF is determined from CT image of the interface between different materials, this method is a suitable choice of the LSF measurement, as it can avoid the weakness of using a wire phantom or phantom that contains metal foil. The procedures which have been carried out to measure the spatial resolution of the system consist of several steps; the first step began with the preparation of the Micro-CT system which provides a direct way to image the phantom to obtain the CT scan image which was used to determine the step function (ESF) as illustrated in Figure 4.

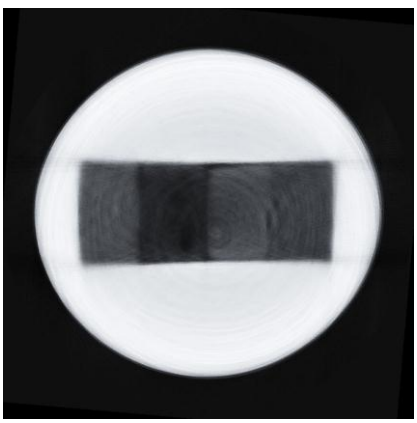

Figure 4: reconstructed CT image of the developed phantom

The second step was saving the image acquired by the system into BMP file format, also known as bitmap image file. It is a format widely used to store the bitmap digital images used for medical information. This image was transferred to a personal computer and was analyzed using the Image processing program (ImageJ 1.50i version) for further processing. The ImageJ software was used to extract the response function or the step function from the obtained image experimentally by taking the line profile cross section (cross-sectional plots), which is acquired at the interface between every two materials as shown in Figure 5. Ten line profiles were extracted between every two materials to obtain the ESF. Those lines profile taken were converted from pixel to (mm) and then normalized to a maximum value for the fitting process with the MATLAB (R2015b) software.

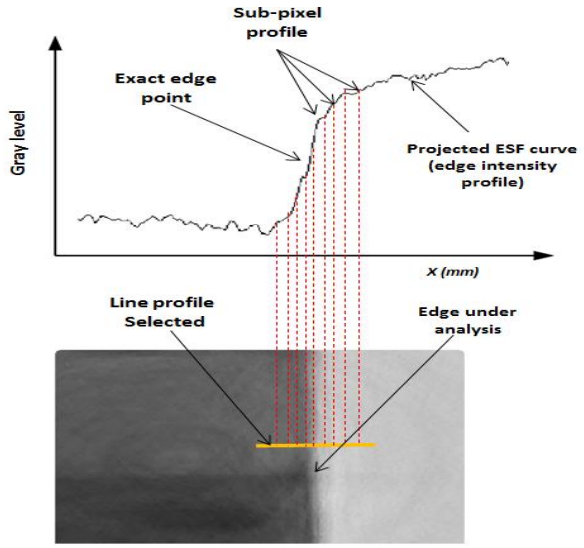

Figure 5: Edge detection regions in the image data using ImageJ software

The third step used MATLAB (R2015b) software for fitting the ESF data to obtain the resolution parameter (λ). The data of every line selected was uploaded to the MATLAB Curve Fitting app by selecting x and y data and then fitted with Mathematical relationship. The value of parameter (λ) resulting from fitting the mathematical expression to the ESF data was used to calculate the spatial resolution using following equation:

$$ESF = \frac{1}{2} + \frac{1}{\pi}\, tan^{-1}\left(\lambda(x - x_0)\right) \quad (1)$$

Where λ is the resolution parameter which determined in the fitting process?

The fourth step was differentiating the outcome of third step using MATLAB to achieve the LSF with respect to x using equation:

$$LSF = \frac{\lambda/\pi}{1 + \lambda^2\,(x - x_0)^2} \quad (2)$$

The narrowness or spread of the LSF in (Eq. 2) was entirely determined by the parameter λ. The LSF width was shown to be inversely proportional to this parameter. The resolution property was illustrated by determining the full-width-at-half-maximum (FWHM) of the LSF. Note that x_0 is an arbitrary coordinate location for the infinitesimally narrow slit. By choosing $x_0 = 0$, it leads to a particularly simple form [26]

$$LSF = \frac{\lambda/\pi}{1 + \lambda^2\, x^2} \quad (3)$$

For the line spread function of (Eq. 3), the x-coordinate corresponds to one-half of the maximum of LSF, to be represented by ($x_{1/2}$) which is a solution of;

$$\frac{1}{2}\left(\lambda/\pi\right) = \frac{\lambda/\pi}{1 + \lambda^2\, x_{1/2}^2} \quad (4)$$

This yields to;

$$x_{1/2} = \frac{1}{\lambda} \quad (5)$$

By doubling the magnitude $\frac{2}{\lambda}$, it will achieve the Full Width at Half Maximum (FWHM).

RESULTS

In the present work, the ESFs data were analyzed at the interface between every two materials in the reconstructed CT image including the background material. This study used CT image of developed phantom shown in Figure. 4, but similar phantom designs are commonly used for the measurement of spatial resolution in CT system. The phantom contained five different materials which were allowed for the measurement of the ESFs at different locations in the image. The ESFs were constructed by extracting a line profile cross-section with a length of 120 equal for all data with region of 141×197 pixels around the edge from the image data as shown in Figure 6, and then following the procedure described previously. The edge was detected in that region using ImageJ software.

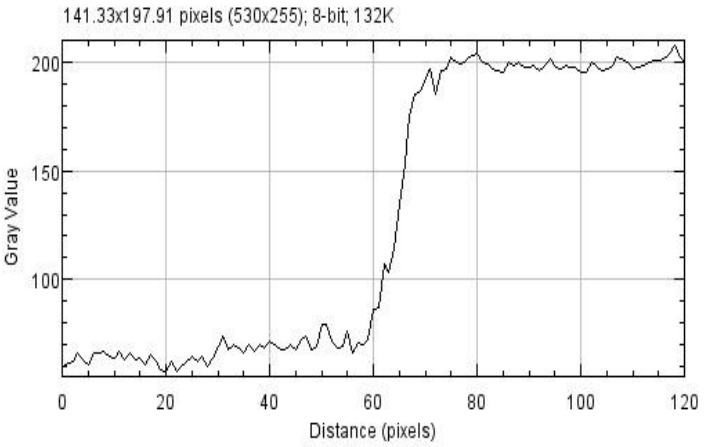

Figure 6: Edge detection data between two materials using ImageJ software

The ESFs collected from the image data were fitted on the mathematical expression shown in Eq.1 using curve fitting

tools box by MATLAB (Version R2015b) to obtain the resolution parameter (λ) of the ESFs. The value of the parameter (λ) achieved from the fitting process of every data was averaged and then differentiated to calculate the LSF. Figure 7 to 13 presents the fitting curves of the ESFs data between every two materials in the CT image.

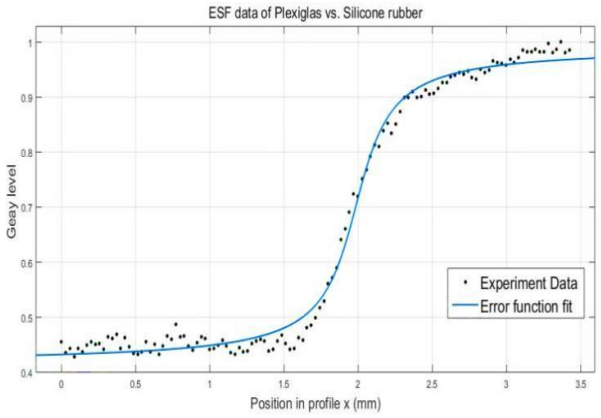

Figure 7: ESF data of Plexiglas vs. Silicone Rubber

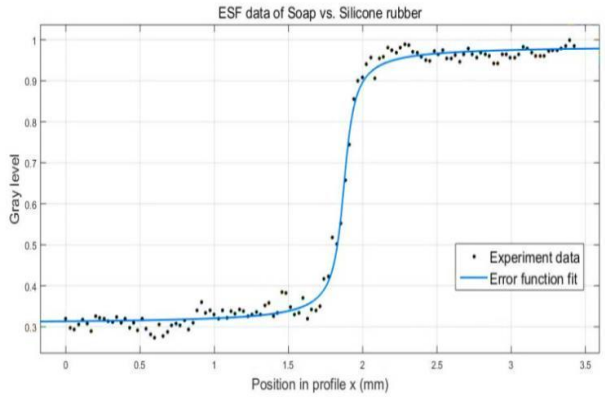

Figure 8: ESF data of soap (Sodium Palmate), vs. Silicone

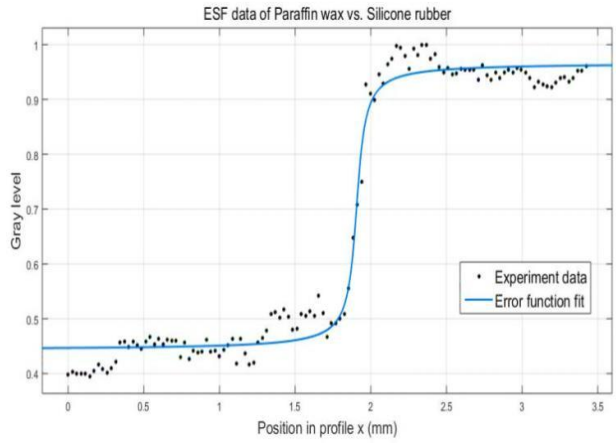

Figure 9: ESF data of paraffin wax vs. Silicone Rubber

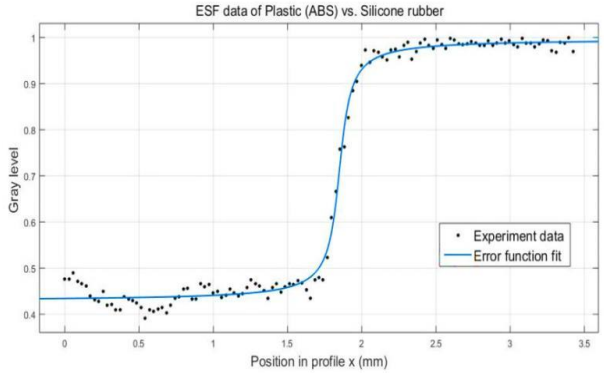

Figure 10: ESF data of plastic (ABS) vs. Silicone Rubber

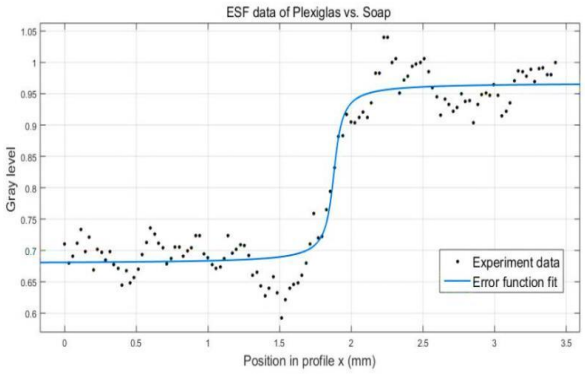

Figure 11: ESF data of Plexiglas vs. soap (Sodium Palmate)

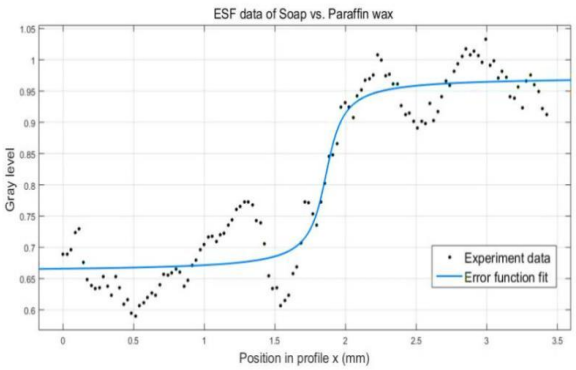

Figure 12: ESF data of soap (Sodium Palmate), vs. paraffin

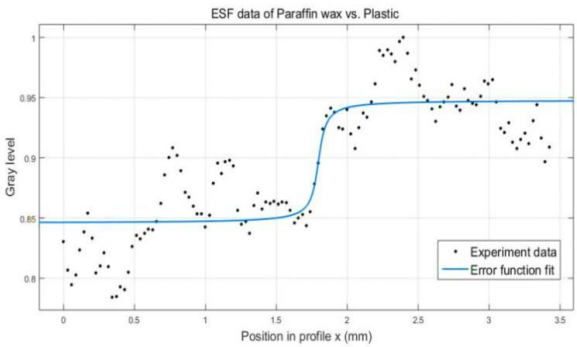

Figure 13: ESF data of paraffin wax vs. plastic (ABS)

The value of (λ) obtained from the fitting function of each ESF selected in the reconstructed CT image is shown in table 1. The differentiation process of the ESF to achieve the LSF was accomplished by simply using first differences. The ESF profile data were established from the CT image within seven different edge locations; they were between every two different materials such as Plexiglas and silicone rubber etc. The differentiation process of the ESF was calculated for the seven edge data within the same CT image to achieve the LSF using the mathematical expression shown in equation 2. A narrow LSF is a much sought goal of a radiographic imaging system like CT. The narrowness or spreading of the LSF was completely determined by the parameter (λ). The resolution property was illustrated by determining the FWHM of the LSF.

Table 1: Resolution parameter and FWHM results

No	Material	Resolution parameter (λ) (1/mm)	FWHM (mm)
1	Plexiglas Vs. Silicone Rubber	9.06 ± 0.07	0.220 ± 0.007
2	Soap Vs. Silicone Rubber	18.53 ± 0.04	0.107 ± 0.002
3	Paraffin wax Vs. Silicone Rubber	21.31 ± 0.06	0.103 ± 0.002
4	Plastic (ABS) Vs. Silicone Rubber	12.28 ± 0.08	0.162 ± 0.006
5	Plexiglas Vs. Soap	8.86 ± 0.23	0.225 ± 0.025
6	Soap Vs. Paraffin wax	9.00 ± 0.08	0.222 ± 0.008
7	Paraffin wax Vs. Plastic	29.96 ± 0.27	0.066 ± 0.009

The term FWHM is used to describe measurement of the width of an object in an image. In other words, it is the width of the LSF curve measured between every two materials within the image obtained from the Micro-CT on the y-axis which are half the maximum amplitude. However, the larger the (λ), the smaller the FWHM obtained, and the narrower the LSF. The high-resolution imaging system was considered by the large values of this resolution parameter. In table 1 the numerical results of the FWHM were calculated with the mathematical expression for several LSF obtained. The plots of the LSF curves which a result of the differentiation process can be seen in Figure 14. The LSF graphs were normalized in this study to evaluate the spatial resolution of the CT system.

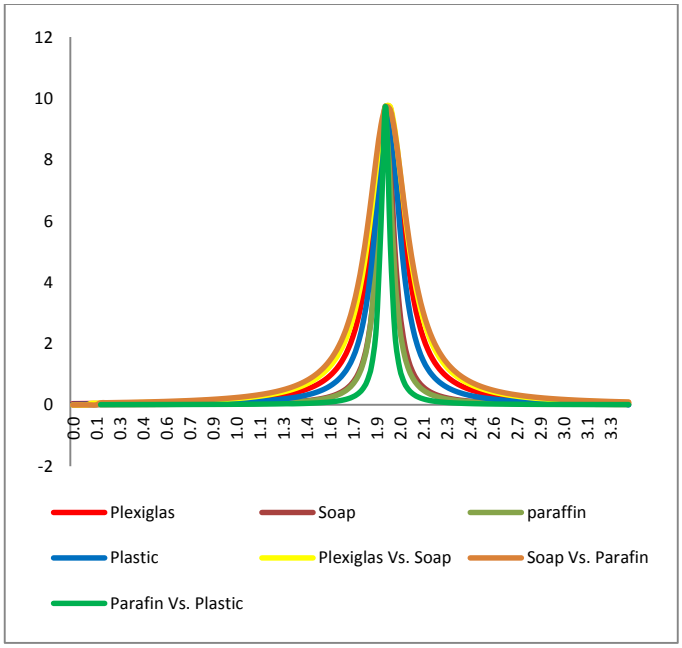

Figure 14: Results of the normalized LSF of the CT image

In order to assess the precision of the measurement method, the results of the repeatability were achieved by following the same experimental procedure used in the main experiment which was aimed to obtain the spatial resolution parameters of the CT system, five scans were taken by removing and replacing the phantom using the same system and the same identical scan parameters, in each scan the CT image was reconstructed and ESFs were obtained for each reconstructed CT image between the component materials of the image. The number of pixel count was also measured in the image at different locations using the same cross-section profile (ImageJ line profile). The results of the repeatability measurements were calculated by the (Paired Samples *t* Test) using SPSS Statistics which was based on the calculating the *P*-value and confidence interval of the difference in detection the accuracy between the main scan and the repeatability scans, we found that the *P* -value obtained is larger than the standard *P* -value. Therefore, we cannot conclude that a significant difference exists.

DISCUSSION

The methodology used in this study was presented to show the capability of evaluating the spatial resolution of the CT system. The obtained results provide a practical measurement of the CT system spatial resolution, which was based on the calculation of the LSF from a related function called the ESF. The ESF data were constructed from the CT image which was obtained by scanning phantom made of silicone rubber shaped as cylindrical containing different materials. On CT machine, materials with very divergent densities are easy to differentiate. In proper conditions, CT machines are able of discriminating the values of linear attenuation coefficient (μ) that differ as little as 0.1%, where is the (μ) values of the materials were used in our phantom achieved by Almahdi

[27]. As a result, increasing the difference in materials density will increase the spatial resolution. Moreover, increasing the difference in the material attenuation coefficients will also enhance the spatial resolution. Clearly, if materials are very different in their attenuation properties, very fine details or very small particles can be imaged, but if they are similar to only larger-scale details and or particles, they can be reliably distinguished [28].

The measurements of the spatial resolution were derived graphically from the value of the FWHM of the LSF. According to McRobbie [29], the FWHM of the experimental LSF can be used as an indicator of the CT system spatial resolution. The LSF was mathematically calculated as the derivative of the ESF by making the determination of either of the functions equally useful. A smooth edge is also easier to achieve than a narrow slit. It gives the ESF an additional practical advantage in comparing with LSF produced from wire method used in the previous studies [22]. Moreover, the data from the number of pixels in the regions of interest (ROI) that were selected to construct the ESF on the CT image were quite enough to implement the new developed methods.

The quality of CT spatial resolution is related to the width of the LSF. The narrowness of the LSF was totally determined by the parameter (λ). The large value of the resolution parameter (λ) was obtained between paraffin wax and plastic (ABS) materials = 29.96±0.27 1/mm, and the FWHM of those materials = 0.066±0.009 mm. The smallest value of the (λ) was obtained between Plexiglas and soap materials = 8.86±0.23 1/mm, and the FWHM = 0.225±0.025 mm, the FWHM results of the other materials were Plexiglas with silicone rubber = 9.06±0.07 mm, soap with silicone rubber = 18.53±0.04 mm, paraffin wax with silicone rubber = 21.31±0.06 mm, and soap with paraffin wax = 9.00±0.08 mm. The measured spatial resolution for the CT images of the constructed phantom utilized was fairly consistent with one another. As shown in our previous measurements, the values of the spatial resolution indicator (FWHM) achieved slightly have differences between the materials on the CT image. The small differences observed in the value of the FWHM were related to the inherent contrast of an object and the sum of the blurring effects including the imaged object itself [30]. As the (λ) between the materials increase, the spatial resolution will increase as well. However, as the FWHM between the materials gets narrower, the spatial resolution will rise instead.

Finally, this work presented an alternative methodology to the measurement of the spatial resolution of Micro-CT machine using developed multi-materials phantom, and the future work will evaluate the spatial resolution of the clinical CT system.

CONCLUSIONS

A newly developed method for the measurement of the spatial resolution of CT system was presented in this paper, based on extracted ESF profile from CT image using recently designed phantom made as a cylindrical shape. The ESF was constructed by extracting a line profile acquired at the interface between different materials which was then fit it with mathematical expression using MATLAB. The proposed method can be applied using data from CT images contained different materials and is not affected by the noise introduced during the differentiation process of the ESF to produce the LSF. In addition, the experiment has indicated that the differentiation of the ESF can provide a precise assessment of the LSF. The proposed method was successfully applied using multi-material phantom images presenting edges between every two materials. The spatial resolution property was derived graphically from the value of the FWHM of the LSF. In addition, in addition, the results of the repeatability measurement test were statistically accepted.

ACKNOWLEDGMENTS:

The author would like to express many thanks to the Libyan Government ministry of education for providing a scholarship.

REFERENCES

[1] Herman, G.T., 1980, Image Reconstruction from Projections: *The Fundamentals of Computerized Tomography*, Academic Press, New York.

[2] Buzug, T., 2008 Computed Tomography: From Photon Statistics to Modern Cone-Beam CT (Springer-Verlag), Berlin, Heidelberg.

[3] Hricak, H., Brenner, D.J., Adelstein, S.J., Frush, D.P., Hall, E.J., Howell, R.W., and McCullough, C.H., 2011, Managing Radiation Use in Medical Imaging: a Multifaceted Challenge Radiology 258 889-905.

[4] Munera, F., Rivas, L.A., Nunez, D.B., Jr., and Quencer, R.M., 2012, Imaging evaluation of Adult Spinal Injuries: Emphasis on Multi Detector CT in *Cervical Spine Trauma Radiology* 263 645-60.

[5] Raja, A.S., Mortele, K.J., Hanson, R., Sodickson, A.D., Zane, R., and Khorasani, R., 2011, Abdominal Imaging Utilization in the Emergency Department: Trends over Two Decades International *Journal of Emergency Medicine* 4 19.

[6] Hsieh, J., 2009, Computed Tomography: Principles, Design, Artifacts, and Recent Advances, 2nd Edition, SPIE, Bellingham.

[7] Holdsworth, D.W., and Thornton, M.M., 2002, "Micro-CT in Small Animal and Specimen Imaging," *Trends in Biotechnology*, vol. 20, no. 8, pp. 34-39.

[8] Lee, S.C., Kim, H.K., Chun, I.K., Cho, M.H., Lee, S.Y., & Cho, M.H,. 2003, A Flat Panel Detector Based Micro-CT: Performance Evaluation for Small Animal Imaging, *Physics in Medicine and Biology*, 48(24), 4173-4185.

[9] Ritman, E.L., 2004, "Micro-Computed Tomography-Current Status and Developments," *Annu Rev Biomed Eng*, vol. 6, pp. 185–208.

[10] Suparta, G.B., Louk, A.C., Sam, N.H., and Wiguna, G.A., 2013, "Quality Performance of Customized and Low Cost X-ray Micro-Digital Radiography System", published in Sirisoonthorn, S.(Editors), 2014. Proc. SPIE 9234, *International conference on Experimental Mechanics, and Twelfth Asian Conference on Experimental Mechanics*, 9234(7 pages).

[11] Bourne, R., 2010, Fundamentals of Digital Imaging in Medicine, 1st edn, Springer, Verlag.

[12] Goldman, 2007, Principles of CT: Radiation Dose and Image Quality', *J Nucl Med Technol*, vol. 35, no. 4, pp. 213-25.

[13] Seeram, E., 2010, *Digital Radiography: An Introduction for Technologists*. Delmar, Cengage Learning.

[14] Romans, L.E., 2011, Computed Tomography for Technologists; a Comprehensive Text, Philadelphia; Wollters KluwerHealth/Lippincott Williams and Wilkins.

[15] Ohkubo M, Wada S, Matsumoto T, Nishizawa K., 2006 An effective method to verify line and point spread functions measured in computed tomography. Med. Phys ; 33:2757–2764. [PubMed]

[16] Rathee S, Fallone BG, Robinson D., 2002 Modulation transfer function of digitally reconstructed radiographs using helical computed tomography. Med. Phys ; 29:86–89. [PubMed]

[17] Rainer, G., Jens, K., and Marek, K., 2008, 'Assessment of Spatial Resolution in *CT' IEEE Nuclear Science Symposium Conference Record* 978-4244 2715-4/08.

[18] Siewerdsen JH, Jaffray DA., 2000 Optimization of x-ray imaging geometry (with specific application to flat-panel cone-beam computed tomography) Med. Phys ; 27:1903–1914. [PubMed]

[19] Rong, J.Y., Guotao, F.U and Cunfeng W.E., 2010, Measurement of spatial resolution of the micro-CT system. Journal of IOP SCIENCE CPC(HEP & NP) 412–416 Chinese Physics Vol. 34, No. 3.

[20] Judy, P.F., 1976, the Line Spread Function and Modulation Transfer Function of a Computed Tomographic Scanner. Medical Physics 3:233-236.

[21] Boone, J. M., 2001, Determination of the Presampled MTF in Computed Tomography, *Med. Phys.* 28, 356-360.

[22] Bentzen, S.M., 1982 Evaluation of the spatial resolution of a CT scanner by direct analysis of the edge response function, Published by the American Association of Physicists in Medicine, Medical Physics 10, 579; doi: 10.1118/1.595328.

[23] ICRU Report No. 87: Radiation dose and image-quality assessment in computed tomography.

[24] Kusminarto, 1986, Study and Development of Techniques in Computerized Tomography, *Thesis Ph.D.*, Surrey University, U.K.

[25] Blumenfeld, S.M., and Glover, G., 1981, Spatial Resolution in Computed Tomography in Radiology of the Skull and Brain, Volume 5. Technical Aspects of Computed Tomography, edited by Newton, T. H and Potts, D.G. Mosby Company, C. V. St. Louis, 3918-3940.

[26] Harms, A.A., and Whyman, D.R., 1986, Mathematical and Physics of Neutron Radiography, D. Riedel Publishing Company Dorderech, Holan.

[27] Almahdi, M., Kus, K., and Gede B. S., 2017, A New Simple Method to Measure the X-ray Linear Attenuation Coefficients of Materials Using Micro-Digital Radiography Machine, *International Journal of Applied Engineering Research* ISSN 0973-4562 Volume 12, Number 21 pp. 10589-10594.

[28] Flannery, B.P., Deckman, H.W., Roberge, W.G., D'Amico, K.L., 1987, *Three-dimensional X-ray microtomography*. Science 237, 1439-1444.

[29] McRobbie, D.W., 1997 "A three-dimensional volumetric test object for geometry evaluation in magnetic resonance imaging," Med. Phys. 24(5), 737– 742.

[30] Bourne, R., 2010, Fundamentals of Digital Imaging in Medicine, 1st edn, Springer, Verlag.